DISCRETE LIMIT ANALYSIS OF PLAIN CONCRETE BEAMS USING RBSM WITH VORONOI MESH DIVISION

Norio TAKEUCHI*

1. INTRODUCTION

RBSM is a numerical analysis method developed as a limit analysis of structures, in which the total structure is idealized as an assemblage of rigid body elements connected by two kinds of distributed springs [1]. This idealization can read the comprehensive expression of discontinuous phenomenon due to cracking and slippage that significantly affects a failure of concrete structures [2] [3]. However, the RBSM solution on failure modes tends to be controlled by its element division, because the strain energy is evaluated along its element boundaries. When the failure mode cannot be included in the mesh division, then the over-estimated solution on collapse loads is obtained [4]. Further, the method requires skill because cracking patterns depend upon the uncertainty in the distribution of the material strength.

Voronoi tessellation was introduced into the element division of RBSM to numerically examine the constitutive relation of materials by TOI et al. [5] The tessellation is directly adopted as element of RBSM that can accept arbitrary polygonal elements. However, it was difficult to make the mesh division of the polygons manually, because they are formed to equalize every territory of their reference points [6]. Thus, the author developed a computer aided system to automatically form the tessellation, using computer-generated, pseudo-random numbers as their reference points.

In this study, the geometry of Voronoi element division by the developed system is examined, and the applicability of RBSM with the Voronoi elements to the discrete limit analysis of plain concrete beams is discussed including the size effect on strength of the beams. The beams to be analyzed are subjected to pure bending, in which the distribution of the material strength affects the initiation and the propagation of cracking.

2. CHARACTERISTICS OF PSEUDO-RANDOM NUMBERS

Pseudo-random numbers generated by computer according to the linear congruence method were used herein as the reference points of Voronoi polygons.

*理工学部土木工学科　教授　計算力学・応用力学

Because the geometry of Voronoi polygons depends upon their reference points to the pseudo-random numbers, those numbers were examined first.

The concept of the fractal, which is a shape with self - similarity, was introduced to quantitatively examine the distribution of the random numbers. The box cutting method was employed as shown in Fig.1. The coupled random numbers were plotted as closed circles, distributed over a square region of side L. The region was then subdivided into square boxes of side l, in which shaded boxes have no circles.

The relation among l/L and the total boxes with the couples were shown in Fig.2 on a logarithmic scale. In this figure, the absolute value of the gradient is the fractal dimension which shows the statistical self - similarity. The fractal of the distribution can be found when the total exceeds 500, since the regression line indicating the fractal dimension could be fairly well drawn. It was decided that more than 500 points of the pseudo - random numbers were uniform enough to be adopted as the reference points.

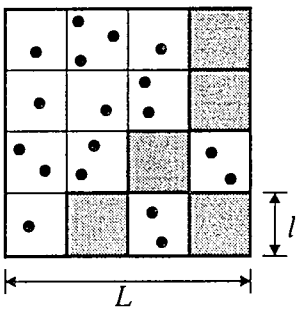

Fig.1 Grid division by square domain

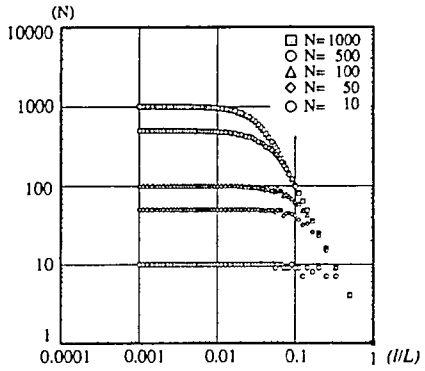

Fig.2 Fractal-curve of random numbers

3. GENERATION OF VORONOI TESSELLATION

Voronoi tessellation can be formed by connecting the circumcentres of the Delaunay triangle network as shown in Fig.3, in which the reference points are used as the apexes of the triangle. The geometry of the polygons is consistent with RBSM formulation, in which strain is evaluated by a finite different scheme with the interval of the length between the centroids of the neighbor elements, because the lines between the centroids of the neighbor polygons cross their boundary lines perpendicularly.

Fig.4 shows an example of the polygons formed with 1000 reference points of random numbers according to the linear congruence method, in which small polygons due to the characteristics of pseudo-random numbers can be seen.

The evaluation on element size is required for nonlinear analysis of concrete

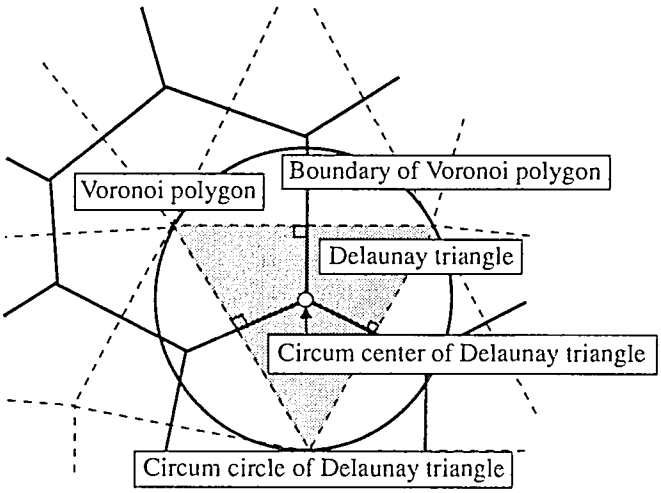

Fig.3 Voronoi tessellations and Delaunay triangles

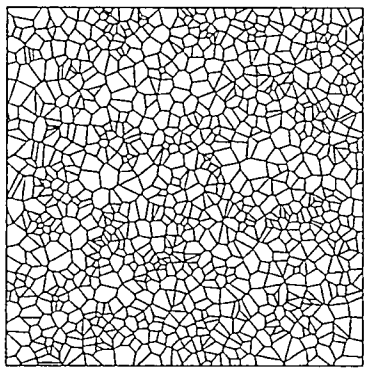

Fig.4 Example of mesh division

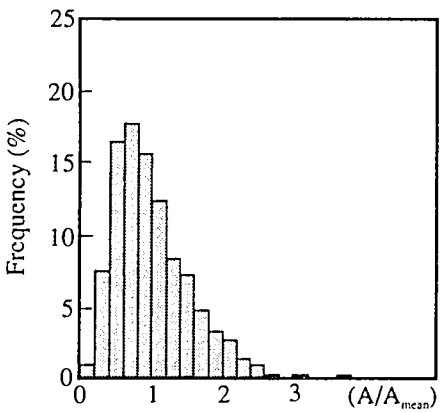

Fig.5 Frequency distribution of element area

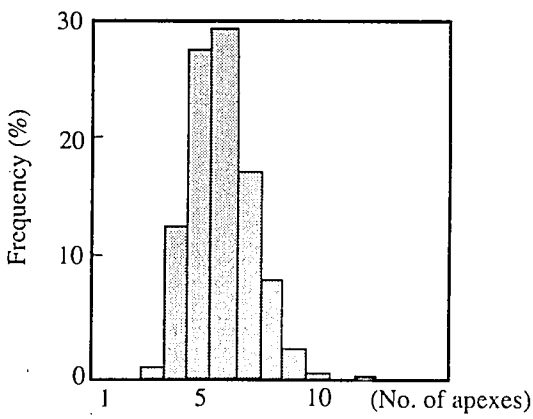

Fig.6 Frequency distribution of number of apexes

structures where the close relationship between crack opening width and fracture energy has been recognized. Therefore, the frequency of the element area was examined as an index of element size.

In Fig.5, the horizontal axis indicates the ratio of an element area A to a mean element area in the percentage of the frequencies. This figure is an example for 1000 reference points of random numbers and their similar tendencies. It shows that the maximum frequency occurred at less than 1 of A/A_{mean}, when the number of the points increased. Fig.6 shows the distribution of the apexes of an element and it can be shown that the major shape was a hexagon, which is generally regarded as stable in nature.

Fig.7 shows the distribution of the lengths and the directions of the element boundaries in Fig.5 in the polar coordinate system, which is an example of when the initial values of the generation were set at 17 and 31.

Fig.8 shows another example of when they were set 1 and 4. Fig.7 shows a uniform distribution, while in Fig.8, obvious orientation to 135 degrees can be found. Thus, attention should be paid to such orientation due to pseudo random numbers.

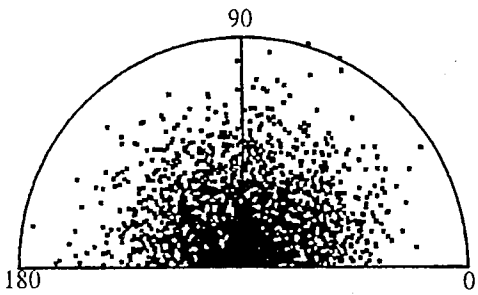

Fig.7 Distribution of the lengths and the directions of the element boundary (non-directional)

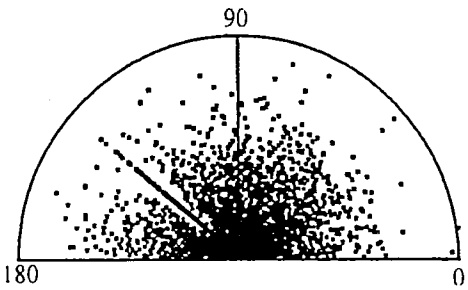

Fig.8 Distribution of the lengths and the directions of the element boundary (directional)

4. CONSTITUTIVE LAW OF CONCRETE

The broken line on Fig.9 shows the uniaxial stress - strain curve of the concrete. In the numerical calculations, this curved line is approximated according to the trilinear solid line. In this paper, F_c being the compressive strength, the first yield level $F_{c1} = 0.5F_c$, the second yield level $F_{c2} = 0.95F_c$, and the reduction ratio of the stiffness $\beta = 0.5$. After the second yielding at ε_{cu} (0.3%), F_{c2} is maintained until collapse. Beyond this point, until reaching $2\varepsilon_{cu}$, the stress decreases with a corresponding increase in the strain, and it stays finally at $0.2F_c$. The tension - softening effect is thereby taken into consideration. The tensile stress is released going along the cubic equation of strain. However, in this study, the linear function connecting with (F_t, ε_t) and $(0, n\varepsilon_t)$, is introduced and n = 40, 20 or 10 are used, considering size effect.

The shearing slippage surface is defined by Mohr - Coulomb's criterion, and after yielding, the associated flow rule is employed, and moves on the surface. Based on the supposition above, Fig.10 shows the yield and collapse surface of

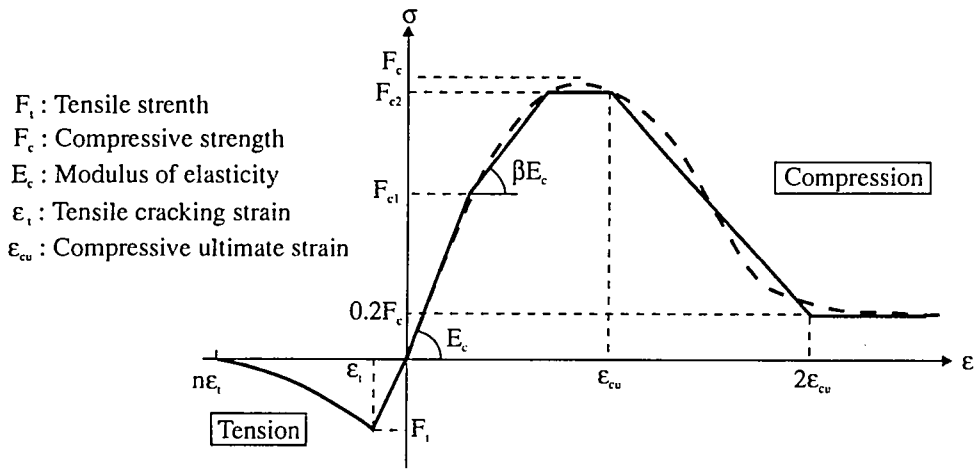

Fig.9 Stress-strain relationship for concrete

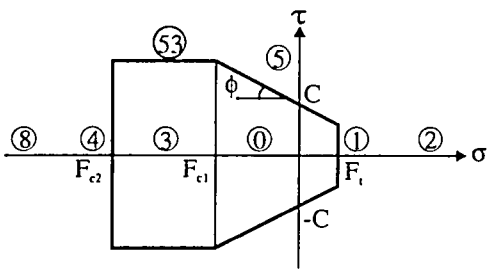

⓪ : Elastic
① : Cracked Unloading
② : Completely Cracked
③ : First Yielding
④ : Second Yielding
⑤ : Shear slip
⑧ : Crushed

Fig.10 Yield and collapse surface for concrete

concrete using RBSM. The state ⓪ shows elasticity, the surface ① is cracking, the state ② is the condition where the residual stresses become zero, in Fig.9, that is a state of tension on the left side from $n\varepsilon_{cr}$. The state ③ shows first yield, the surface ④ shows second yield, and the state ⑧ is the normal strain having the condition reached at the strain limit ε_{cu} of Fig.9. The surface ⑤ shows shear slipping. After this state, in the case where first yield compression of the state ③ has occurred, the state follows the stage in the surface ⑬.

5. NONLINEAR ANALYSIS ALGORITHM

In concrete structures, shapes change as cracking develops, and then stress is released on the cracking surface. The released stress or load leads to a decline of convergence of solutions near and at the ultimate stage of loading. To overcome this condition, we proposed an algorithm for material nonlinear analysis [3] [10], in which r_{min} method [9] was modified to add the released force to the remaining load while counting the applied load, and to simultaneously take into account the slip, cracking and compressive failure.

However, the algorithm is to be originally applied to an incremental load method. This method is inadequate to simulate the crack propagation in detail, because the failure of plain concrete beams under bending is brittle. The algorithm can also be applied to an incremental displacement method if the incremental displacement is taken as external force. Thus, the following nonlinear analysis was carried out according to an incremental displacement method.

6. ANALYSIS OF PLAIN CONCRETE BEAMS

Using RBSM with Voronoi elements, the analyses of the plain concrete beams as shown in Fig.11 were carried out to examine the size effect. Three beams with different heights were analyzed. Specimen No.1, No.2 and No.3 had 5cm, 10cm and 20cm heights respectively. Further, two cases of element divisions were used. One had almost the same elemental area for each specimen, and the other had the same number of elements.

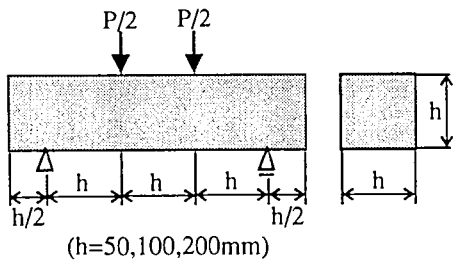

Fig.11 Analyzing model of plain concrete beam

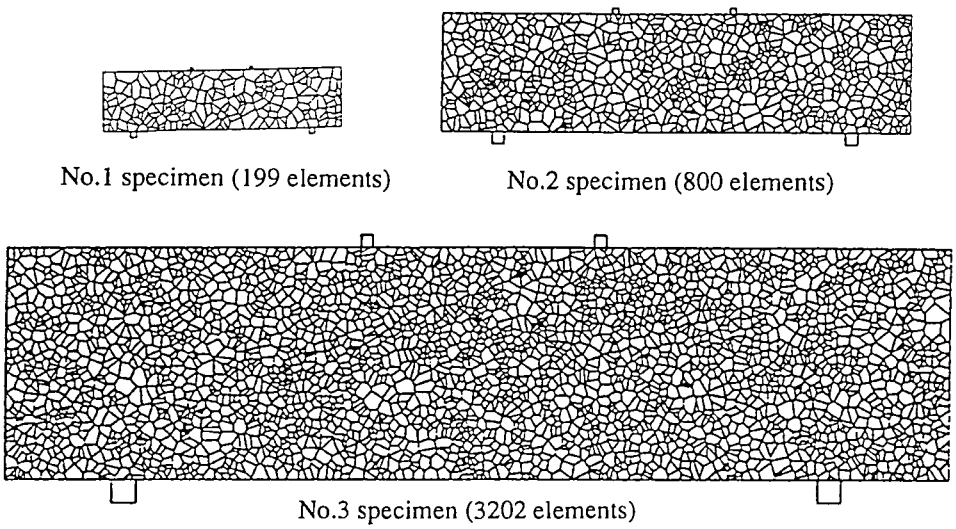

Fig.12 Voronoi elements of a plain concrete beam (same average area)

6.1 Numerical example with same areas of Voronoi elements

The element divisions for all specimens were made to have almost the same average areas, about 1cm^2, and number of elements were about 200, 800 and 3200 respectively, for No.1, No.2 and No.3. Moreover, another element division for all specimens were also prepared with the different initial values of the random number for element generation. Fig.13 is an example of element divisions. Table 1 shows the material constants used. Those values and the critical tensile strain of $20\varepsilon_t$ in strain softening curve evaluated by fracture energy were commonly used for all specimens.

An example of crack propagation is shown in Fig.13, in which several initial cracks were observed in and around pure bending regions, and then they grew

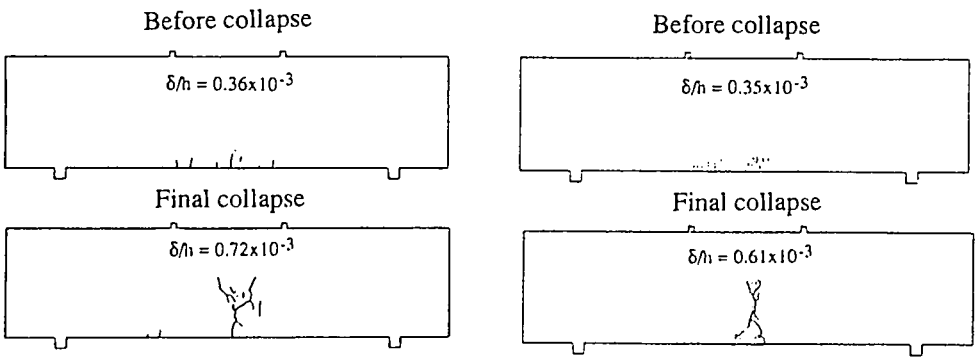

(a) No.2 specimen (800 elements)

(b) No.3 specimen (3202 elements)

Fig.13 Crack patterns of plain concrete beam(same average area)

Table 1. Material property constants of concrete

Compressive strength (F_c)	34.3 MPa
Tensile etrength (F_t)	2.9 MPa
Cohesive strength (c)	4.7 MPa
Angle of friction (ϕ)	37.0 deg.
Modulus of elasticity (E_c)	27.5 GPa
Poisson's ratio (ν)	0.2

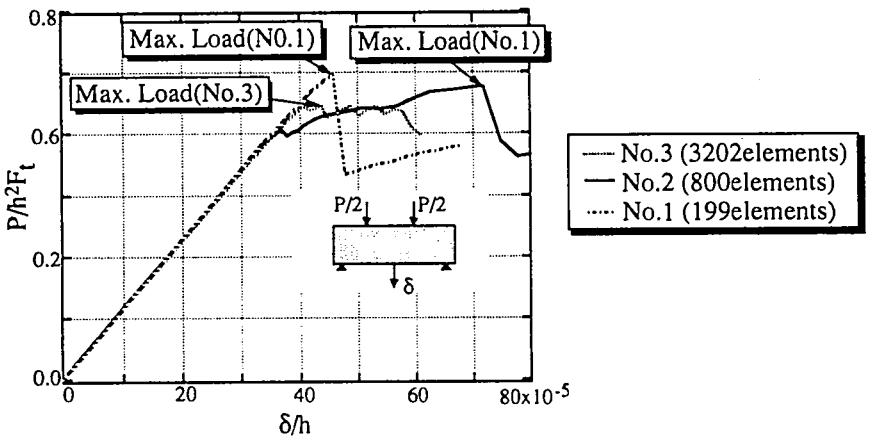

Fig.14 Load-Displacement relation (same element area)

Table 2. Maximum load (with the same area)

Specimen	Number of elements	Max.Load (kN)	$P/(h^2F_t)$
No.1	199	3.74	0.50
	200	4.19	0.56
No.2	800	13.8	0.48
	798	14.1	0.49
No.3	3202	51.6	0.45
	3198	49.3	0.42

gradually, and consequently, a major crack in tension was formed which caused the structural collapse.

The load carrying capacities and the relations between applied load and dis-

placement are shown in Table 2 and Fig.14, respectively.

In these examples where an identical strain softening curve was used, the solutions of these specimens with different heights, both on the crack propagation and the normalized strength, were somewhat different. When the specimen size was longer, the P/h^2F_t value decreased as shown in Fig.17. This shows the size effect.

6.2 Numerical example with the same number of Voronoi elements

To analyze the specimens with the same number of elements, the element divi-

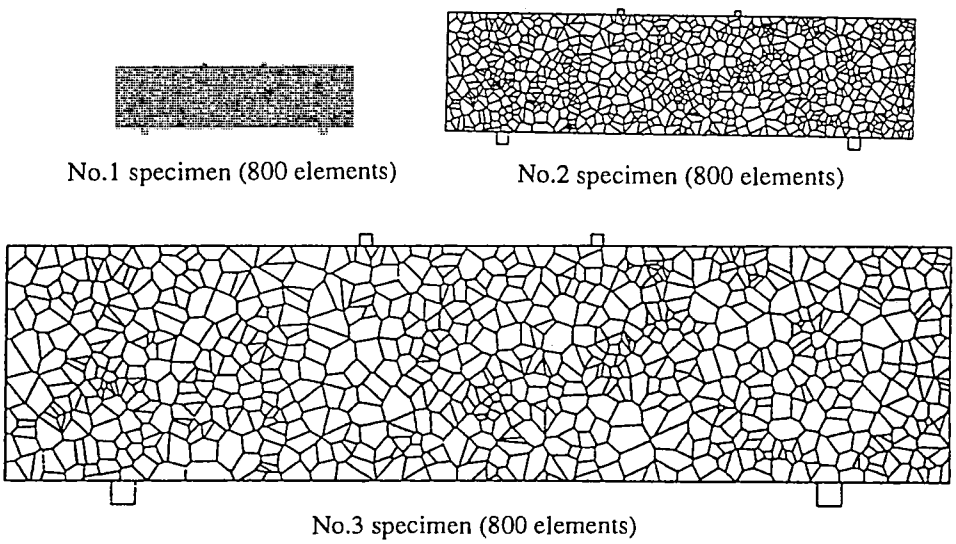

Fig.15 Voronoi elements of plain concrete beam (same number of elements)

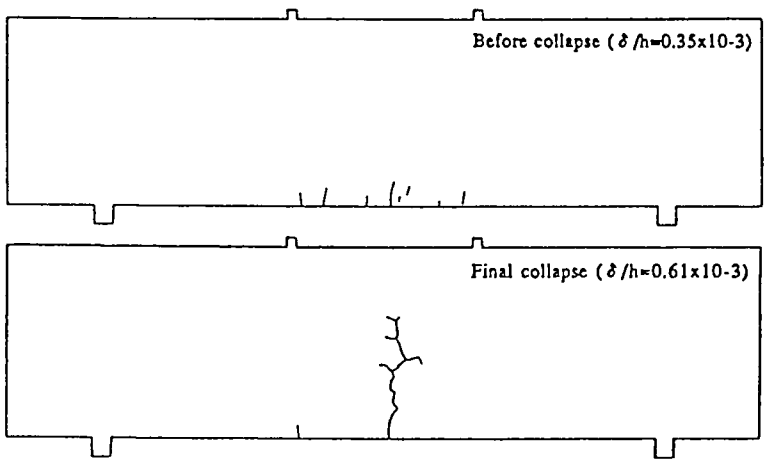

Fig.16 Crack patterns of plain concrete beams (the same number of element)

sion for No.2 was made as shown in Fig.15. In the case of No.3 specimen, the critical tensile strain in the strain-softening curve was set at $10\varepsilon_t$, and in case of No.1 it was set at $40\varepsilon_t$. Other constants were the same as Table 1.

Fig.16 shows the crack propagation for specimen No.2, and the load carrying capacities for both are also listed in Table 3. The differences on the former between two specimens was slight, while that of the latter was enough to show the size effect, which was probably caused by that of the strain-softening curve in tension.

The numerical results obtained in this section are plotted in Fig.17, in which the vertical and the horizontal axis are bending strength and beam height, respectively, and the lines also show the experimental results. This figure shows that the degradation of the strength for a higher specimen due to size effect was observed numerically.

Table 3. Maximum load (with same number of element)

Number of elements	Specimen	Max.Load (kN)	$P/(h^2F_t)$
800	No.1	4.3	0.57
	No.2	13.8	0.48
	No.3	44.7	0.39
798	No.1	4.4	0.58
	No.2	14.1	0.49
	No.3	43.3	0.37

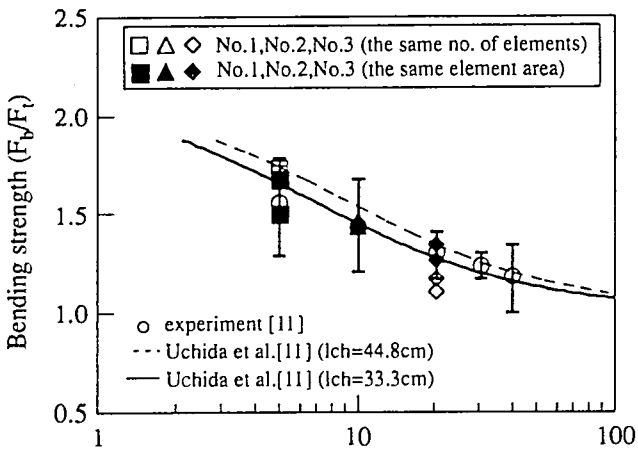

Fig.17 The height of beam-bending strength relationship

7. CONCLUSIONS

The collapse analysis of plain concrete beams has been carried out by using RBSM with an automatic mesh generating system of Voronoi polygons. The conclusions obtained are as follows:

1) The fractal of the random numbers generated by computer according to the linear congruence method was observed when the total numbers exceeded 500. It could be analogically judged to guarantee the fractal of more than 500 Voronoi polygons based on the random numbers.
2) The validity of RBSM with Voronoi elements has been verified for the non-linear analysis of concrete structures up to failure including discontinuous phenomenon due to cracking, even if the failure mode could not be presumed.
3) The size effect of concrete structures could be considered when the strain - softening curve under tension was defined by fracture energy.

The size effect has been generally recognized to be caused by the reasons that follow:

1) Concrete is not homogenous and there is a probability of how the strength and the defect will be distributed.
2) Shrinkage varies with the size of the concrete member.

It should be required to examine concrete from a microscopic viewpoint, to see if the size effect can be observed numerically when the defect and the strength are distributed according to a probability along the boundaries of Voronoi elements.

REFERENCES

[1] Kawai,T. : New element models in discrete structural analysis, J. of the Society of Naval Architects of Japan, No.141,pp187-193,1977
[2] Kawai,T. et al. : Discrete limit analysis of reinforced concrete structures (1-3), SEISAN - KENKYU, Monthly J. of Institute of Industrial Science, Univ. of Tokyo, Vol.38,No.4-6,1986 (in Japanese)
[3] Kawai,T. et al. : Application of a discrete limit analysis to reinforced concrete shear panels,Proc. 2nd World Congress on Computational Mechanics, August 27-31,1990,Stuttgart,FRG,pp862-865.1990
[4] Takeuchi,N. and Kawai,T. : On the error evaluation of the solutions obtained by the new discrete limit analysis,Proc. of 15th Symposium on Matrix method, pp77-82,1981 (in Japanese)
[5] Toi.Y. et al. : Mesoscopic simulation of microcracking behaviors of brittle polycrystalline materials,ISAN - KENKYU, Monthly J. of Institute of Industrial Science, Univ. of Tokyo, Vol.42,No.7,pp444-447,1990 (in Japanese)
[6] Iri,M. (Supervision) : Computational geometry and geographical information process, Kyoritsu Pub.,1993 (in Japanese)

[7] Takeuchi,N et al. : On the automatic mesh generation for RBSM by using Voronoi tesselation, Proc. of the JSCE 48th annual meeting, Part I,pp1430-1431,1993 (in Japanese)
[8] Fushimi,M. : Random numbers, Univ. of Tokyo Press, Tokyo, 1989 (in Japanese)
[9] Yamada, Y. et al. : Plastic stress-strain matrix and its application for the solution of elasto-plastic problems by a finite element method, Int. J. of Mechnical Science, Vol.10,pp343-354,1968
[10] Takeuchi,N. and Kawai,T. : A discrete limit analysis of granular materials including effects of the solid contact, US-Japan seminar, MICROMECHANICS OF GRANULAR MATERIAL, October 26-30, SENDAI, ZAO, pp116-125 (1987)
[11] Uchida,Y et al. : Application of fracture mechanics to size effect on flexiral strength of concrete, Proc. of JSCE,No.442,pp101-107,1992 (in Japanese)